JTTEE5 14:61-66
DOI: 10.1361/10599630522710
1059-9630/$19.00 © ASM International

Intermediate Temperature Solid Oxide Fuel Cell Based on Fully Integrated Plasma-Sprayed Components

X.Q. Ma, H. Zhang, J. Dai, J. Roth, R. Hui, T.D. Xiao, and D.E. Reisner

(Submitted August 12, 2003; in revised form February 2, 2004)

This work addresses the fabrication of membrane-type solid oxide fuel cells (SOFCs) operating at medium temperatures, where all components are fabricated by plasma spray technology, and the evaluation of the performance of the SOFC single unit in a temperature range of 500 to 800 °C. Single cells composed of $LaSrMgO_3$ cathodes, $LaSrGaMgO_3$ (LSGM) electrolytes, and Ni/yttria-stabilized zirconia anodes were fabricated in successive atmospheric plasma-spraying processes. Plasma-spraying processes have been optimized and tailored to each layer to achieve highly porous cathode and anode layers as well as high-density electrolyte layers. A major effort has been devoted to the production of the LSGM electrolyte that has a high density and is free of cracks. Electrochemical impedance spectroscopy was used to investigate the conductivity of the electrode layers, and particularly the resistance of the electrolyte layer. It revealed that the heat treatment had a great influence on the specific conductivity of the sprayed electrolyte layers and that the specific conductivity of the heat-treated layers was dramatically increased to the same magnitude as is typical for sintered LSGM pellets. The experimental results have demonstrated that the plasma-spraying process has a great potential for the integrated fabrication of medium-temperature SOFC units.

Keywords intermediate temperature, $LaSrGaMgO_3$ electrolyte, plasma spray, solid oxide fuel cell

1. Introduction

Solid oxide fuel cells (SOFCs) are capable of generating electric power with high efficiency through the chemical reaction between hydrocarbon fuels H_2 and CO, resulting from the reforming of hydrocarbon fuels. However, for technical application, mechanical and electrochemical reliability has to be improved, and the present production costs has to be reduced. Both can be achieved by reducing the cell operating temperature (Ref 1-4). Therefore, the development of an intermediate-temperature SOFC technology has attracted a lot of worldwide research and development activities for future energy markets. As related to SOFC technology, a lower operating temperature requires higher electrode activity, ionic conductivity of electrolytes, lower overpotential at the electrode/electrolyte interface, and lower overall internal resistance loss. These requirements can be met through developing new electrode/electrolyte materials and new cell assembly concepts, as well as novel fabrication methods (Ref 5, 6).

The original version of this article was published as part of the ASM Proceedings, *Thermal Spray 2003: Advancing the Science and Applying the Technology*, International Thermal Spray Conference (Orlando, FL), May 5-8, 2003, Basil R. Marple and Christian Moreau, Ed., ASM International, 2003.

X.Q. Ma, H. Zhang, J. Dai, J. Roth, R. Hui, T.D. Xiao, and **D.E. Reisner,** US Nanocorp, Inc., 74 Batterson Park Rd., Farmington, CT 06032. Contact e-mail: xma@USNanocorp.com.

The plasma-spraying technique has been developed and adapted to the specific requirements of membrane-type SOFC fabrication in a consecutive and cost-effective spray process. Atmospheric plasma spraying (APS), vacuum plasma spraying (VPS), radio frequency plasma spraying (RFPS), and high-velocity oxyfuel (HVOF) spraying have demonstrated their capability to produce dense electrolyte layers as well as porous electrode layers (Ref 7-11). Of the thermal spray technologies, VPS has been considered to be highly promising for producing thin and dense electrolyte layers consisting of yttria-stabilized zirconia (YSZ) in most cases, and APS and RFPS for forming porous electrode layers. The authors have addressed the use of an inexpensive and universal APS system for the integrated fabrication of dense electrolyte and porous electrode layers for a medium-temperature SOFC unit. From the view point of the technical issues associated with high-density electrolyte deposition by APS, it is quite possible to fabricate high-density electrolyte layers by APS if a new electrolyte material is available. Recently, strontium- and magnesium-doped $LaGaO_3$ perovskite oxide (LSGM) has been proposed as a possible electrolyte material for medium-temperature SOFCs (Ref 12-15). LSGM material has two major favorite properties for the thermal spray forming of dense electrolyte films. (a) It has a high oxygen ion conductivity of 0.1 S/cm at 800 °C (i.e., four times higher than that of YSZ). As a result, it enables the application of a slightly thicker LSGM electrolyte film, for which a usual thickness of 100 to 200 μm is needed to ensure gas tightness and to get enough power density at a medium temperature. (b) LSGM has a much lower melting point (~1600 °C) than that of YSZ (~2380 °C). With such a low melting point, APS can produce quite high-density films, just as in the case of dense dielectric films such as Al_2O_3/TiO_2. Beyond the benefit of cost savings, some technical advantages also have been identified with the plasma-spraying process.

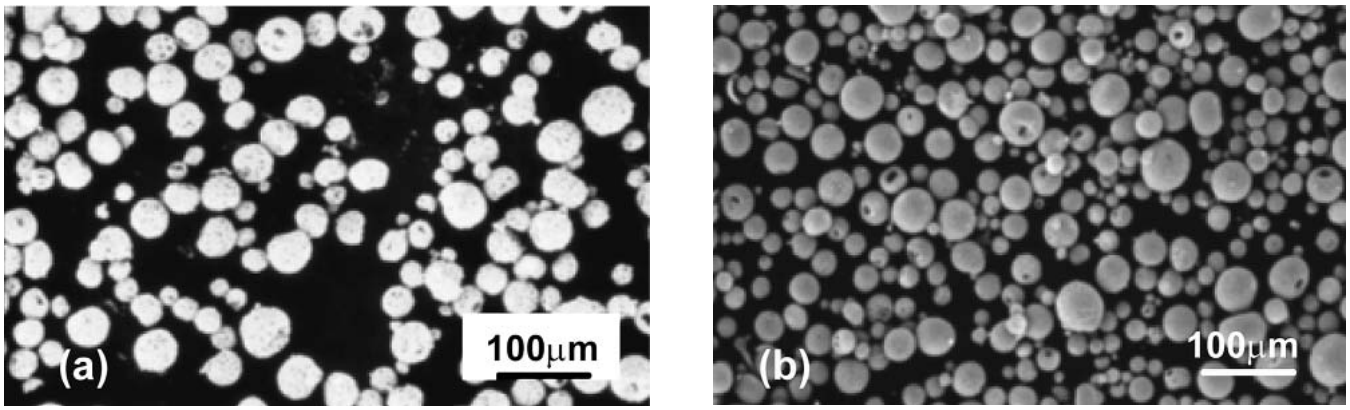

Fig. 1 The SEM morphologies of LSM (a) and LSGM (b) powder feedstock

For example, with the conventional "cofiring" process for cell fabrication, the reaction has been performed at 1470 °C between the electrode and electrolyte in the $LaSrMgO_3$ (LSM)/LSGM system, and the formation of a solid solution between these two materials at 1270 °C also was reported (Ref 16). Obviously, the sintering-induced reaction/degradation phenomenon can be eliminated in a plasma-spraying process.

This article deals with an intermediate-temperature SOFC system that consists of an LSM cathode, an LSGM electrolyte, and Ni/YSZ anode layers applied by air plasma spraying. The single SOFC unit was tested and evaluated at medium temperatures of 500 to 800 °C, and the phase composition and polarization resistance of those layers were correlated to spray conditions and also operating temperature.

2. Experimental Details

2.1 Materials

The feedstock materials used were $La_{0.8}Sr_{0.2}MnO_3$ (Praxair Specialty Ceramic, Woodinville, WA) and $La_{0.8}Sr_{0.2}Ga_{0.8}Mg_{0.2}O_3$ (Praxair Specialty Ceramic) for cathode and electrolyte, respectively. Both materials have a purity of 99.9%, and a size distribution of D_{50} 39.4 μm for LSM and D_{50} 36.9 μm for LSGM, as shown in Fig. 1(a) and (b). The anode material is Ni/50YSZ, which was prepared by the mechanical mixing of the two components.

2.2 Cell Fabrication

Planar cells were fabricated by the sequential air plasma spraying of LSM cathodes, LSGM electrolytes, and Ni/YSZ anodes. The Sulzer Metco (Westbury, NY) plasma spray system equipped with a 9 MB gun was used to apply those layers. Argon was used as the primary working gas, and the typical spray parameters included: (a) for anode layers, 500A/65V, spray distance (SD): 15 cm, 2268 g/h; (b) for cathode layers, 700A/32V, SD: 15 cm, 907 g/h; and (c) for electrolyte layers, 650A/55V, SD: 9 cm, 907 g/h.

2.3 Cell Test Setup

The cell test system consists of a furnace with an Al_2O_3 ceramic tube chamber, H_2 and O_2 gas supply units, an exhaust unit, and an electronic measurement unit. The typical hydrogen flow rate was 0.02 standard liter per minute. The basic electronic unit includes a high-resistance multiple meter (>1G Ohm), a current meter, and an adjustable resistance. For the electrochemical evaluation of the cells, a computer-based alternating current impedance test system was used. Also, open-circuit voltage (OCV) values and voltage-current density curves were taken to obtain impedance spectra in the temperature range of 500 to 800 °C. In addition, x-ray diffraction (XRD) and SEM techniques have been used for identifying the phase compositions and microstructures of those sprayed deposits.

3. Results and Discussion

3.1 Cathode Layer

The microstructure of a plasma-sprayed LSM cathode layer was examined in cross section by SEM and is shown in Fig. 2. Obviously, highly porous layers could be produced for the cathodes. The porosity can be related to two facts under the optimized spray condition: (a) predominantly, to the presence of numerous unmelted or partially melted particles and (b) to the formation of gas pores indicated by the presence of closed spherical pores formed at a relative low coating temperature. Because the cathode layer acts as oxygen/air electrode, the high-porosity structure is desirable for providing multiple paths for air transportation to the cathode/electrolyte interface. Thus, air plasma spraying is believed to be an effective and efficient method for producing highly porous LSM cathode layers.

The phase compositions of the starting LSM feedstock and the spray deposits were analyzed by XRD. In Fig. 3, the XRD patterns indicate that the LSM material before and after spraying only consists of a single phase, which means that there is no major phase transformation under the spray condition. The only change is found with the peak broadening for the LSM deposit that indicates the formation of a fine grain structure by the plasma-spraying process.

3.2 Electrolyte Layer

The LSGM electrolyte layer was plasma-sprayed onto the LSM cathode layer, and its microstructure is exhibited in Fig. 4.

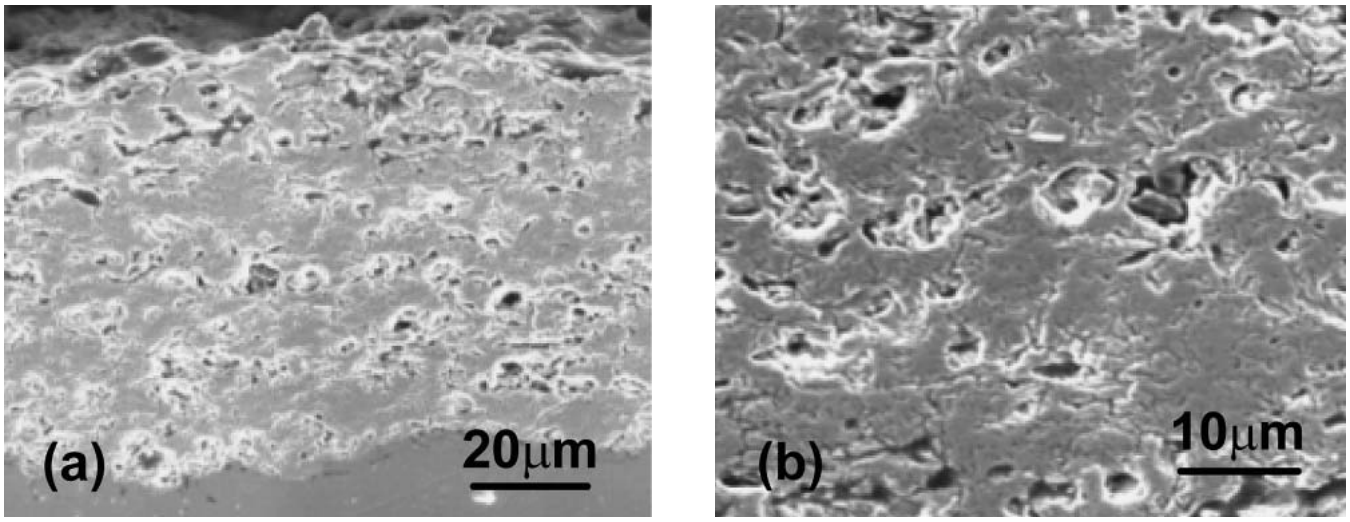

Fig. 2 Microstructural graphs of the as-sprayed LSM cathode film, which is generally porous (a) and includes some unmelted particles and gas pores (b)

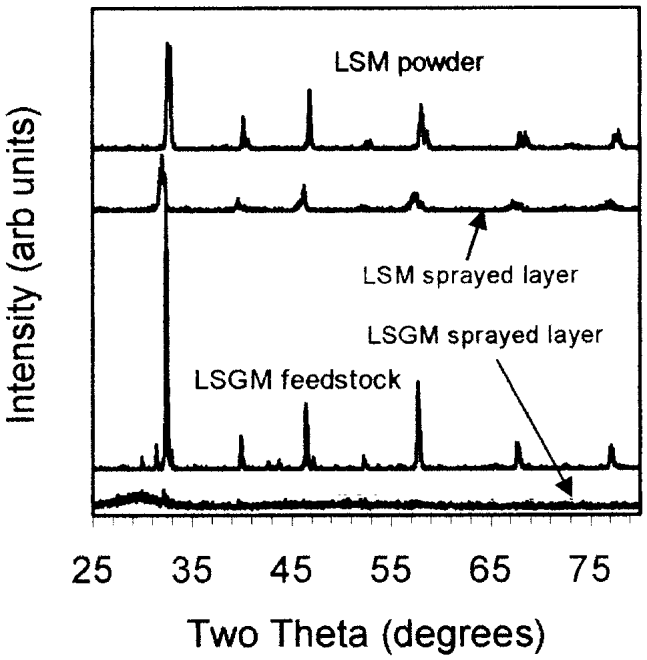

Fig. 3 XRD analyses for LSM and LSGM feedstock powders and as-sprayed deposits. There is no phase transformation for LSM, but an amorphous LSGM phase is obtained due to the spraying process.

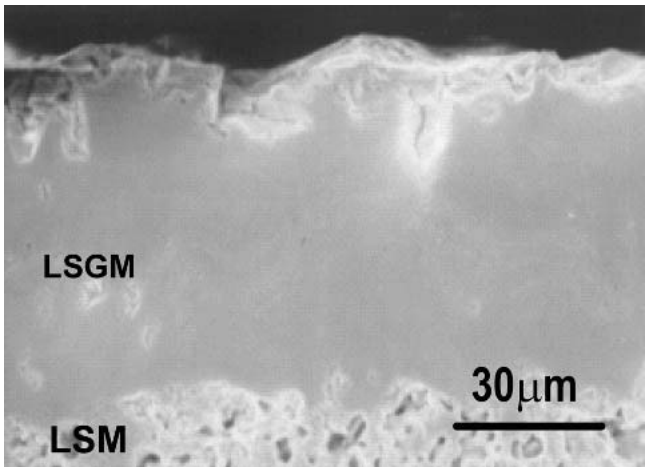

Fig. 4 A cross section of the as-sprayed LSGM electrolyte layer, indicating a high coating density

In general, the electrolyte layer is formed with a high density, a uniform thickness, and satisfactory interfacial connection with the porous LSM substrate. The main defects are the isolated pores, which probably can be attributed to the inclusion of some unmelted large-size particles. Normally, the electrolyte layer is 100 to 150 μm thick; however, the process is capable of also producing thin layers of 50 μm thickness, while keeping the microstructure, continuity, and uniformity of the deposit under the optimized plasma condition.

The XRD analysis was conducted for the starting LSGM feedstock and the as-sprayed deposit, and the XRD patterns are also shown in Fig. 3. The LSGM powder was identified as being of a single phase, but the as-sprayed LSGM layer was identified by amorphous phases, which was indicated by the severely broadened peaks. To investigate the transition temperature for the crystallization of the sprayed LSGM deposit, it was exposed to post-heat-treatment at temperatures rising in steps from 100 to 900 °C. In Fig. 5, the XRD data show that the LSGM deposit starts to crystallize when the heat treatment temperature exceeds 500 °C, and a high degree of crystallization is identified above 700 °C. The formation of the amorphous phase is due to the rapid quenching of droplets in the plasma-spraying process. As a general phenomenon, the quenching effect may result in the growth of fine grains (e.g., the LSM layer) or amorphous phase formation to some extent (e.g., the LSGM layer). Some studies have revealed that the crystallization of some perovskite oxides such as LSM greatly depends on the oxygen partial pressure of the

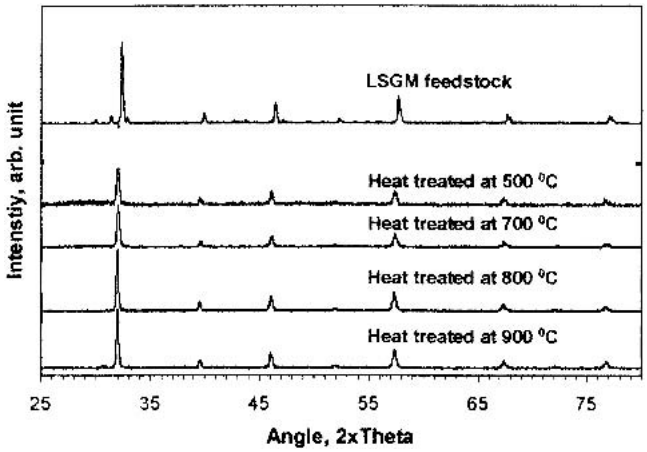

Fig. 5 The XRD patterns for the sprayed LSGM electrolyte layer after heat treatment at different temperatures. The crystallization of the amorphous phase takes place above 500 °C, and a complete transition is achieved at some 700 °C.

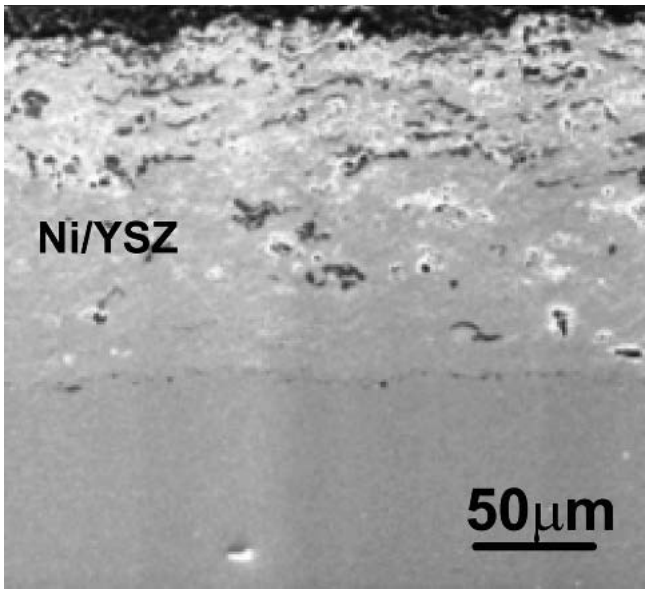

Fig. 6 The SEM microstructure of the as-sprayed porous Ni/YSZ anode layer

spray environment in which LSM can release oxygen at temperatures considerably above 1400 °C (Ref 17, 18). From the point of oxygen ion conductivity, the formation of the amorphous phase in the LGSM layer is definitely negative. Fortunately, the XRD data confirmed that the chemical stoichiometry for the deposit was not altered (i.e., there is no observable decomposition occurring in the spray process), and full crystallization can be achieved with post-heat-treatment at medium temperatures.

3.3 Anode Layer

The Ni/YSZ anode layer is shown in cross section in Fig. 6. The overall anode layer is porous, and numerous microscopic

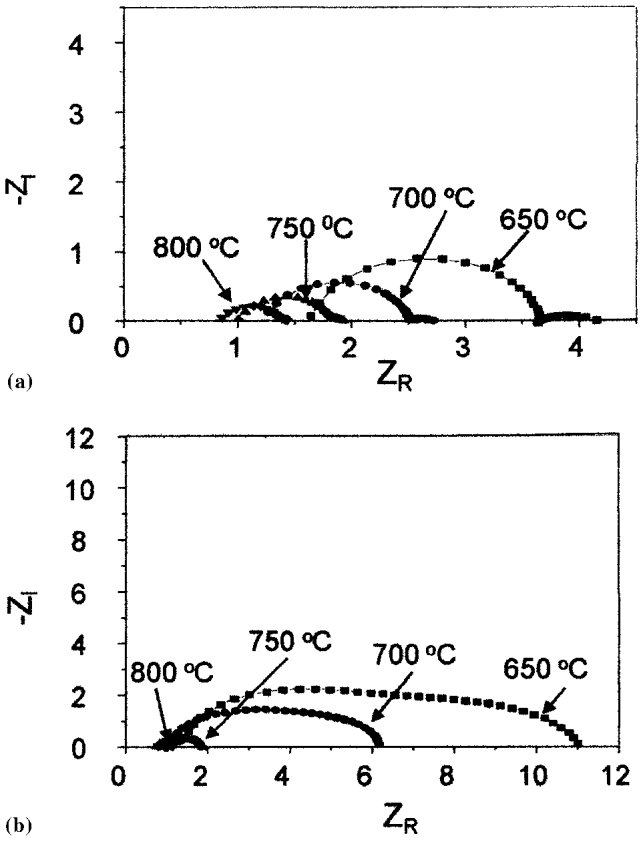

Fig. 7 Electrochemical impedance spectra for the as-sprayed LSGM deposit (a) and sintered LSGM pellet (b) tested at temperatures between 650 and 800 °C

and macroscopic pores can be observed. The composition analysis by energy dispersive x-ray spectroscopy (EDAX) indicates that Ni and YSZ components are distributed uniformly through the whole layer thickness. When the Ni/YSZ anode layer is applied on the LSGM electrolyte, a well-adhering layer can be achieved usually.

3.4 Electrochemical Evaluation

To investigate the polarization resistance of the plasma-sprayed LSGM electrolyte, a freestanding LSGM pellet 10 mm in diameter was prepared. In addition, for comparison LSGM pellets sintered at 1450 °C for 20 h were also produced. Both, the sprayed and sintered pellet samples were pasted on two sides with Pt-black glue, and Pt foils were used as connecting leads to the pellets. The electrochemical impedance spectroscopy technique was applied to measure the resistance/conductivity at temperatures of 500 to 800 °C in air. Figure 7 shows the electrochemical impedance spectra for the sprayed (a) and sintered (b) LSGM samples. Consequently, the resistance R of the electrolytes and specific conductivity data estimated with an equivalent circuit method are listed in Table 1. The specific conductivity of the plasma-sprayed pellet is much lower than that of the pellet sintered below 750 °C. However, when the sintering temperature was increased to over 750 °C, the specific conductivity of the plasma-sprayed electrolyte was close to that of the sintered

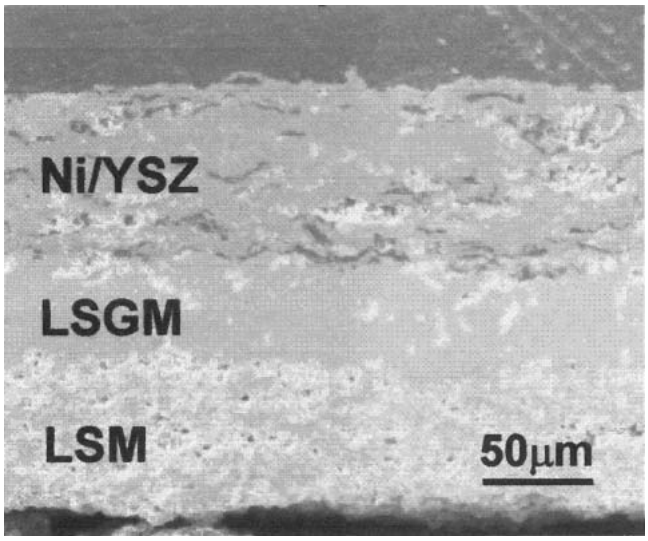

Fig. 8 A typical microstructure of a sprayed single cell consisting of LSM cathode, LSGM electrolyte, and Ni-YSZ anode

Table 1 Resistance and conductivity comparison of as-sprayed and sintered LSGM pellets at several temperatures

Temperature, °C	Resistance (*R*), Ohm	Specific conductivity, S/cm
Plasma-sprayed LSGM layer		
650	311	0.000225
700	340	0.000206
750	1.11	0.0631
800	0.82	0.0854
Sintered LSGM pellet		
650	1.3	0.0641
700	1.2	0.0694
750	0.76	0.110
800	0.75	0.111

pellet. This result reveals that the plasma-sprayed LSGM pellet undergoes a significant change in structure at around 750 °C, which is consistent with the XRD data indicating a complete crystallization above 700 °C.

Furthermore, the electrochemical impedance spectrum of the sprayed LSGM film exposed to a heat treatment at 800 °C for 0.5 h was examined. The data given in Table 2 exhibit a dramatic increase in the specific conductivity of the sprayed LSGM after heat treatment, which is comparable to that of the sintered counterpart at similar temperature values. The above results show that the conductivity of the as-sprayed LSGM electrolyte can be significantly improved through total crystallization by a suitable heat treatment. Therefore, air plasma spraying can be identified as a practical and cost-effective process for performing the deposition of high-conductivity LSGM electrolyte films.

3.5 Single-Cell Performance Evaluation

Single cells comprising of LSM cathodes, LSGM electrolytes, and Ni-YSZ anodes have been fabricated by air plasma spraying. The microstructure of one cell is shown in Fig. 8, in which the thickness of the electrolyte layer is typically 50 to 80 μm. The electrical performance of the cell was evaluated by measuring the OCV and voltage-current density dependency in the temperature range of 500 to 800 °C. Figure 9 presents the results of OCV, 0.95 V at 600 °C and 1.045 V at 700 °C. The OCV of the cell is quite the same as that reported for similar cell systems (Ref 15, 19, 20). The OCV data indicate that the plasma-sprayed electrolyte layer has satisfactory gas tightness to separate hydrogen and air effectively. The power density was measured as 80 to 150 mW/cm^2 at the tested temperatures. Currently, work is being devoted to improve the electrode performance for increasing cell power density.

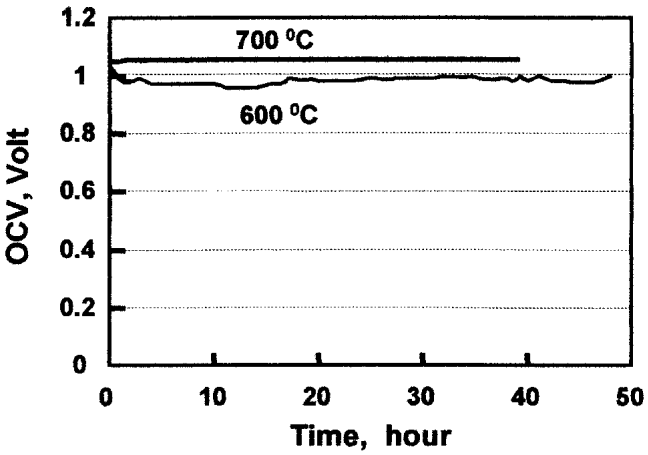

Fig. 9 Profiles of OCV versus time measured with a single cell at 600 and 700 °C with H_2/O_2 fuel

Table 2 Resistance and specific conductivity of sprayed LSGM layer after heat treatment at 800 °C

Temperature, °C	Resistance (*R*), Ohm	Specific conductivity, S/cm
650	1.70	0.412
700	1.26	0.0556
750	1.00	0.0701
800	0.82	0.0854

4. Conclusion

A membrane-type single SOFC unit has been fabricated by cost-effective air plasma spray technology. The cell consists of an LSM cathode/LSGM electrolyte/Ni-YSZ anode, which is fabricated for operation in a medium temperature range from 500 to 800 °C. The microstructural investigation confirmed that porous electrode and dense electrolyte layers were obtained by the air plasma-spraying process, and that single cells were fabricated by consecutive plasma spray processing. The as-sprayed LSGM electrolyte mostly contained amorphous phase; however, a high degree of crystallized LSGM could be achieved by heat treatment at a temperature above 700 °C. The electrochemical impedance spectra indicated that the fully crystallized LSGM electrolyte has a high conductivity that is comparable to

a sintered LSGM pellet. With a good gas tightness of the dense LSGM electrolyte, a cell OCV at close to the theoretical value was measured. These results demonstrate that plasma spray processing is cost-effective and highly promising for the integrated fabrication of medium-temperature SOFC units.

Acknowledgment

US Nanocorp gratefully acknowledges support by the U.S. Department of Energy under grant No. DFFG 02-01ER83340.

References

1. A.J. Appleby, Fuel Cell Technology: Status and Future Prospects, *Energy,* Vol 21, 1996, p 521-653
2. S.C. Singhal, Science and Technology of Solid-Oxide Fuel Cells, *MRS Bull.,* Vol 25, 2000, p 16-21
3. M.C. Williams, Status of Solid Oxide Fuel Cell Development and Commercialization in the U.S., *Proc. Sixth Int. Symp. on Solid Oxide Fuel Cells,* S.C. Singhal and M. Dokiya, Ed., Electrochemical Society, 1999, p 3
4. J.P.P. Hujismans, F.P.F. Van Berkel, and G.M. Christie, Intermediate Temperature SOFC: A Promise for the 21st century, *J. Power Sources,* Vol 71, 1998, p 107-110
5. P. Charpentier, P. Fragnaud, D.M. Schleich, and E. Gehain, Preparation of Thin Film SOFCs Working at Reduced Temperature, *Solid State Ionics,* Vol 135, 2000, p 373-377
6. L.L. Gauckler, K. Sasaki, A. Mitterdorfer, M. Godickemeier, and P. Bohac, Processing of SOFC Ceramic Components, *First European SOFC Forum,* U. Bossel, Ed., 3-7 Oct (Lucerne), European Electrochemistry Society, Vol 2, 1994, p 545-566
7. L.J.H. Kuo, S.D. Vora, and S.C. Singhal, Plasma Spraying of Lanthanum Chromite Films for Solid Oxide Fuel Cell Interconnection Application, *J. Am. Ceram. Soc.,* Vol 80, 1997, p 589-593
8. H. Tsukuda, A. Notomi, and N. Hisatome, Application of Plasma Spraying to Tubular-Type Solid Oxide Fuel Cells Production, *J. Thermal Spray Technol.,* Vol 9, 2000, p 364-368
9. T. Jansing, R. Fleck, J. Decker, and C. Verpoort, Separation and Insulating Layers of Atmospheric Plasma-Sprayed Ceramics for High Temperature Fuel Cells: Development and Implementation, *Tagungsband Conference Proceedings,* (Düsseldorf, Germany), March 17-19, 1999, E. Lugsheider and R.A. Kammer, Ed., DVS Deutscher Verband für Schweißen, 1999, p 69-75
10. G. Schiller, R. Henne, M. Lang, R. Ruckdaschel, and S. Schaper, Development of Vacuum Plasma Sprayed Thin-Film SOFC for Reduced Operating Temperature, *Fuel Cells Bull.,* Vol 3, 2000, p 7-12
11. K. Okumura, Y. Aihara, S. Ito, and S. Kawasaki, Development of Thermal Spraying-Sintering Technology for Solid Oxide Fuel Cells, *J. Thermal Spray Technol.,* Vol 9, 2000, p 354-359
12. T. Ishihara, H. Matsuda, and Y. Takita, Doped $LaGaO_3$ Perovskite Type Oxide as a New Oxide Ionic Conductor, *J. Am. Chem.,* Vol 116, 1994, p 3801-3803
13. M. Feng, B. J. Goodenough, K. Huang, and C. Milliken, Fuel Cells with Doped Lanthanum Gallate Electrolyte, *J. Power Source,* Vol 63, 1996, p 47-51
14. K. Huang, M. Feng, B.J. Goodenough, and C. Milliken, Electrode Performance Test on Single Ceramic Fuel Cells Using as Electrolyte Sr- and Mg-doped $LaGaO_3$, *J. Electrochem. Soc.,* Vol 144, 1997, p 3620-3624
15. X. Zhang, S. Ohara, H. Okawa, R. Maric, and T. Fukui, Interactions of a $La_{0.9}Sr_{0.1}Ga_{0.8}Mg_{0.2}O_{3-\delta}$ Electrolyte with Fe_2O_3, Co_2O_3 and NiO Anode Materials, *Solid State Ionics,* Vol 139, 2001, p 145-152
16. W. Wang and E.E. Hellstorm, *Mater. Res. Soc. Symp. Proc.,* Vol 411, 1996, p 261
17. S. Hui, X. Q. Ma, J. Broadhead, H. Zhang, J. Roth, A. Decarmine, and T. D. Xiao, SOFC Components and Method of Manufacture Thereof, U.S. Patent 601361, 184 (filed on February 28, 2002)
18. Z. Li, Perovskite La $_{1-x}$ $Sr_xMnO_{3-\delta}$ als Kathodenwerkstoff für Hochtemperatur Brennstoffzelle: Pulverherstellung, Beschichtung und Charakterisierung, July Report, 1992 (in German)
19. Z. Li, W. Mallener, L. Fuerst, D. Stover, and F. Scherberich, Plasma Sprayed Perovskite of the Composition $La_{1-x}Sr_xMnO_{3-\delta}$: Phase Analysis and Electrical Conductivity, *Thermal Spray Coatings: Research, Design, and Applications* (Anaheim, CA), June 7-11, 1993, C.C. Berndt and T.F. Bernecki, Ed., ASM International, 1993, p 343-346
20. K. Huang, J. Wan, and J.B. Goodenough, Increasing Power Density of LSGM-Based Solid Oxide Fuel Cells Using New Anode Materials, *J. Electrochem. Soc.,* Vol 148, 2001, p A788-A794
21. T. Fukui, S. Ohara, K. Murata, H. Yoshida, K. Miura, and T. Inagaki, Performance of Intermediate Temperature Solid Oxide Fuel Cells with La(Sr)Ga(Mg)O_3 Electrolyte Film, *J. Power Sources,* Vol 106, 2002, p 142-145